AJNR

Dynamic Changes in Long-Standing Multiple Sclerosis Revealed by Longitudinal Structural Network Analysis Using Diffusion Tensor Imaging

Hui-Qin Zhang, Jacky Chi-Yan Lee, Lu Wang, Peng Cao, Koon-Ho Chan and Henry Ka-Fung Mak

AJNR Am J Neuroradiol published online 1 February 2024
http://www.ajnr.org/content/early/2024/02/01/ajnr.A8115

Published February 1, 2024 as 10.3174/ajnr.A8115

ORIGINAL RESEARCH
ULTRA-HIGH-FIELD MRI/IMAGING OF EPILEPSY/DEMYELINATING DISEASES/INFLAMMATION/INFECTION

Dynamic Changes in Long-Standing Multiple Sclerosis Revealed by Longitudinal Structural Network Analysis Using Diffusion Tensor Imaging

Hui-Qin Zhang, Jacky Chi-Yan Lee, Lu Wang, Peng Cao, Koon-Ho Chan, and Henry Ka-Fung Mak

ABSTRACT

BACKGROUND AND PURPOSE: DTI can be used to derive conventional diffusion measurements, which can measure WM abnormalities in multiple sclerosis. DTI can also be used to construct structural brain networks and derive network measurements. However, few studies have compared their sensitivity in detecting brain alterations, especially in longitudinal studies. Therefore, in this study, we aimed to determine which type of measurement is more sensitive in tracking the dynamic changes over time in MS.

MATERIALS AND METHODS: Eighteen patients with MS were recruited at baseline and followed up at 6 and 12 months. All patients underwent MR imaging and clinical evaluation at 3 time points. Diffusion and network measurements were derived, and their brain changes were evaluated.

RESULTS: None of the conventional DTI measurements displayed statistically significant changes during the follow-up period; however, the nodal degree, nodal efficiency, and nodal path length of the left middle frontal gyrus and bilateral inferior frontal gyrus, opercular part showed significant longitudinal changes between baseline and at 12 months, respectively.

CONCLUSIONS: The nodal degree, nodal efficiency, and nodal path length of the left middle frontal gyrus and bilateral inferior frontal gyrus, opercular part may be used to monitor brain changes over time in MS.

ABBREVIATIONS: AD = axial diffusivity; EDSS = Expanded Disability Status Scale; FA = fractional anisotropy; IFGoperc = inferior frontal gyrus, opercular part; MD = mean diffusivity; MFG = middle frontal gyrus; NAWM = normal-appearing WM; ORBsupmed = superior frontal gyrus, medial orbital part; RD = radial diffusivity; SPMS = secondary-progressive MS

Multiple sclerosis is the most prevalent CNS inflammatory demyelinating disease[1] and poses a great threat to the quality of life for patients and their caregivers. DTI, a diffusion model, has frequently been used to explore WM microstructural abnormalities in MS conditions.[2,3] Widely used diffusion measurements include fractional anisotropy (FA), mean diffusivity (MD), axial diffusivity (AD), and radial diffusivity (RD).[4] Microstructural damage can develop in both the lesion area[5] and normal-appearing WM (NAWM)[6] in MS. According to accumulating evidence from current research,[7,8] FA in lesions often decreases and MD, AD, and RD increase due to demyelination and axonal injury. Similarly, though to a lesser extent, FA in the NAWM also shows a reduction, and MD, AD, and RD are often elevated.[9] However, research on longitudinal microstructural alterations in MS during the follow-up period is limited.

DTI can also be processed by using a network-based approach[10] that maps the topological organization of the brain. Structural networks have provided new insights into the pathologic processes of MS.[11] One of the advantages of graph theory network analysis is that it supports the axonal tension hypothesis,[12] which can reflect the information transfer and neuroplasticity of the brain.[13] The commonly used network measurements are the nodal degree, nodal efficiency, nodal path length, and nodal clustering coefficient.[10] Several recent studies have reported structural DTI network disruption in different subtypes of MS, such as relapsing-remitting MS,[14] secondary-progressive MS (SPMS),[15] and primary-progressive MS,[15] compared with that in healthy controls. For example, Shu et al[16] reported disrupted topological efficiency in MS in terms of reduced global and nodal efficiency compared with those in healthy controls. The clinical relevance of these network measurements has also been reported in previous studies[17,18]; more specifically, Hawkins et

Received August 17, 2023; accepted after revision November 27.

From the Department of Diagnostic Radiology (H.-Q.Z.), National Cancer Center/Cancer Hospital, Chinese Academy of Medical Sciences and Peking Union Medical College, Beijing, China; Department of Diagnostic Radiology (H.-Q.Z., P.C., H.K.-F.M.), Li Ka Shing Faculty of Medicine, Alzheimer's Disease Research Network (H.K.-F.M., K.-H.C.), State Key Laboratory of Brain and Cognitive Sciences (H.K.-F.M.), University of Hong Kong, Hong Kong SAR, China; Department of Medicine (J.C.-Y.L., K.-H.C.), Queen Mary Hospital, Hong Kong SAR, China; and Department of Health Technology and Informatics (L.W.), Hong Kong Polytechnic University, Hong Kong SAR, China.

Please address correspondence to Peng Cao, Department of Diagnostic Radiology, Li Ka Shing Faculty of Medicine, University of Hong Kong, Hong Kong SAR, China; e-mail: caopeng1@hku.hk

Indicates article with online supplemental data.

http://dx.doi.org/10.3174/ajnr.A8115

al[17] observed that reduced network efficiency could impact multiple cognitive domains in MS, and Welton et al[18] proved that network disruption may serve as a major determinant of cognitive deficits in MS. Charalambous et al[19] proved that structural network disruption measurements could explain disability. However, studies on longitudinal structural DTI network alterations in MS are limited.

Though abundant cross-sectional DTI research on MS focusing on either conventional diffusion measurements or structural network measurements has been published in the past decades, few studies tried to explore whether network measurements or diffusion measurements are more sensitive to detect abnormalities in MS. Research in comparing their sensitivity in longitudinal DTI studies is imperative to probe the brain changes in MS. The conventional diffusion measurements are more vulnerable to the crossing or diverging fibers,[4] while the network measurements may not be, so we hypothesize that the network measures would be superior to capture the brain alterations in MS during the follow-up.

Hence, the main objective of this longitudinal study was to track brain microstructural alterations and brain network changes in MS during a short-term follow-up period of 1 year and then to compare which kind of measurement is more sensitive to capture brain changes over time in MS.

MATERIALS AND METHODS

Participants

This longitudinal study was authorized by the local institutional review board, and written informed consent was obtained from all patients. Eighteen patients with MS were recruited for this 1-year longitudinal investigation from the Clinic of the Department of Medicine of the University of Hong Kong from November 2017 to February 2020. All patients with MS were diagnosed according to the latest revised McDonald criteria,[20] and the clinical phenotype classification was based on the latest Lublin criteria.[21] The exclusion criteria were as follows: 1) patients who had claustrophobia or contraindications for MR imaging, 2) patients who had other severe disorders that caused neurologic abnormalities in addition to MS, and 3) patients who were pregnant.

All patients underwent physical examination, neurologic testing, and MR imaging at 3 time points: baseline (t1), at 6 months (t2), and at 12 months (t3). All clinical assessments were performed by the same neurologist during the same week as the MR imaging examinations. The Expanded Disability Status Scale (EDSS) was used to assess physical disability.

MR Imaging Acquisition

MR imaging was performed at the University Imaging Center by using a 3T scanner (Achieva, Philips Healthcare) with a 32-channel head coil. All participants underwent MR imaging at the 3 time points. The MR imaging protocol included 3D T1-weighted MPRAGE (TR = 6.8 ms, TE = 3.2 ms, TI = 900 ms, matrix = 256 × 256 mm, FOV = 240 × 256 × 204 mm, slice thickness = 1.2 mm), 3D T2-weighted FLAIR (TR = 4800 ms, TE = 266 ms, TI = 1650 ms, matrix = 512 × 512, FOV = 250 × 250 × 184 mm, slice thickness = 0.56 mm), and DTI (TR = 3900 ms, TE = 810 ms, matrix = 80 × 80, FOV = 230 × 90 × 230 mm, slice thickness = 3 mm). DTI was performed by using a single-shot, spin–echo EPI sequence with a nonzero b-value ($b = 1{,}000$ s/mm^2) along 15 diffusion-encoding gradient directions. Postcontrast (gadolinium) T1WI was acquired at each time point to determine whether the lesions were active or inactive. The total scanning time was 37 min.

WM Lesion and NAWM Mask

WM Lesion Segmentation. 3D T2-weighted FLAIR WM lesions were identified and automatically segmented for each patient at each time point by using the Lesion-Prediction Algorithm[22] implemented in the Lesion Segmentation Toolbox,[23] version 3.0.05, and run in Statistical Parametric Mapping, version 12 (SPM12; http://www.fil.ion.ucl.ac.uk/spm/). All produced lesion maps were visually checked and manually corrected to ensure that no errors occurred. The lesion mask that referred to the all voxels of all lesions identified after WM lesion segmentation was also produced.

Brain Segmentation. Brain segmentation was carried out by using the Computational Anatomy Toolbox, version 12.6 (CAT12), run with SPM12 implemented in MATLAB R2020a version 9.8.0 (MathWorks). To avoid tissue segmentation bias, lesion-filling was first conducted for MPRAGE images, with the average intensity of surrounding NAWM via "lesion-filling" implemented in Lesion Segmentation Toolbox.[24] Then, the brain was segmented into 3 classes: GM, WM, and CSF, and the WM mask was automatically generated. NAWM masks were obtained by subtracting the lesion mask from the whole WM mask.

DTI Diffusion Measurements Analysis

DTI data were preprocessed by using the FMRIB Software Library (http://www.fmrib.ox.ac.uk/fsl).[25] In the preprocessing steps, the parametric maps (FA, MD, AD, and RD) were derived. The details are provided in the Online Supplemental Data. Then b0 images were transformed into native MPRAGE space.[26] The derived transformation was applied to FA, MD, AD, and RD maps. Then, the measurement values were obtained by using "fslmeants," part of FMRIB Software Library (https://fsl.fmrib.ox.ac.uk/fsl/fslwiki/Fslutils),[25] by using the abovementioned masks.

Structural WM Network Analysis

Node definition. Node and edge were 2 essential components of structural network. Details of the structural WM network analysis are provided in the Online Supplemental Data. Node definition was performed through the following procedures by using SPM12: 1) MPRAGE and b0 first underwent re-origin to make the subsequent co-registration much more accurate; 2) MPRAGE was linearly co-registered to the native b0 image, and the transformation obtained was N; 3) MPRAGE was nonlinearly normalized to the ICBM152 T1 template in the standardized Montreal Neurological Institute space. The transformation matrix produced was M, and the inverse transformation matrix obtained was M^{-1}; and 4) M^{-1} and N were applied to 90 regions derived from the Automated Anatomical Labeling (https://omictools.com/aaltool)[27] atlas in the Montreal Neurological Institute space. Then, the brain was divided into 90 regions in the native diffusion space, which represented the nodes of the brain network.

Table 1: Demographic and clinical characteristics of MS

	MS			
	Baseline	6 Months	12 Months	*P* Value
Sample size	18	18	18	NA
Female:male	13:5	13:5	13:5	NA
Age (yr)	39.11 ± 13.03	39.61 ± 13.03	40.11 ± 13.03	NA
Duration (yr)	12.78 ± 8.53	13.28 ± 8.53	13.78 ± 8.53	NA
EDSS	3.94 ± 2.25	3.94 ± 2.25	4.03 ± 2.18	.633

Note:—NA indicates not applicable. The continuous measurements are presented as mean ± standard deviation. EDSS did not show significant changes during the follow-up period. Duration: the time since initial diagnosis of MS.

This node definition method has been adopted in previous research.[16,28,29] The parcellation quality of the b0 image is provided in the Online Supplemental Data.

WM Tractography. After preprocessing, DTI was applied to the Diffusion Toolkit[30] for deterministic tractography. For the tractography setting, the Fiber Assignment by Continuous Tracking[31] algorithm was applied; the FA threshold of tracking was set between 0.2 and 1, and the turning angle was 45°, which indicated that if the FA value was <0.2 or the turning angle of the fiber was >45°, the tractography would terminate automatically.[32] These settings have been commonly used in previous studies.[16,29,33,34]

Edge Definition. The edges represent the structural connections between 2 separate GM regions. A threshold value of the edge connection was needed to be set to reduce false-positive connections caused by noise and the limitations of tractography. In this study, a threshold of 3 (fiber bundles) was used, which indicated that 2 pair regions were considered connected only if more than 3 fibers existed between them. This threshold value has been commonly used in previous studies.[16,34]

Network Construction. The UCLA Multimodal Connectivity package (https://github.com/jbrown81/umcp) was used to measure the structural connections between between 2 regions. A structural WM network was established for each participant at each time point. Network measurements, including the nodal degree, nodal efficiency, nodal path length, and nodal clustering coefficient, were computed by using the GRaph thEoreTical Network Analysis toolbox (GRETNA).[35]

Statistical Analysis

All statistical analyses were performed by using SPSS Statistics Version 25 (IBM) and GraphPad Prism version 8.0.0 for Windows (GraphPad Software). Statistical significance was set at $P < .05$ in all analyses. The normality of the continuous data distribution was tested by using the Shapiro-Wilk test.

Repeated-measures ANCOVA was applied to quantify longitudinal changes in DTI and network measurements assuming normal distribution and equal variance, wherein the measurements served as a within-subject variable, and age and sex were the confounders. The Bonferroni method was used in the subsequent post hoc pair-wise analysis for these variables. Sphericity was a necessity for data distribution in repeated-measures ANCOVA. The Greenhouse-Geisser method was adopted when sphericity could not be satisfied, as determined by the Mauchly test. When neither normal distribution nor equal variance assumptions were satisfied, the nonparametric Friedman test method was used. The false discovery rate was used to correct for multiple comparisons.

To explore the relationship between these measurements of all brain nodes and EDSS, a series of correlation analyses were first conducted to select the significant regions with EDSS. The left and right nodes were averaged as 1 node (we did not differentiate between the left and right hemispheres, and the measurement values of the left and right hemispheres of the same node were averaged). All the significant regions, age, and sex together were then put into the stepwise linear model to select the significant predictor of EDSS.

RESULTS

Demographic and Clinical Characteristics

All the enrolled 18 patients with MS (15 relapsing-remitting and 3 SPMS) completed the MR imaging scanning and clinical assessment at the 3 time points. The demographic and clinical characteristics of the patients are presented in Table 1. The duration, the time since initial diagnosis of MS, was also provided.

All patients received disease-modifying drugs at the beginning of the study. Two patients with RRMS and 3 patients with SPMS showed worsening during the follow-up period. The details of the patients are presented in Online Supplemental Data. The EDSS scores did not change significantly (Table 1).

DTI Measurements and Association with EDSS

We observed that FA of lesion was smaller than that of NAWM, while MD, AD, and RD of lesion was larger than that of NAWM across all subjects and time points (Online Supplemental Data). However, all DTI measurements of the lesion and NAWM remained stable over time, as shown in the Online Supplemental Data. There was no significant association among the diffusion measurements of the lesions, NAWM, and EDSS.

Structural WM Network Measurements

Longitudinal changes in the significant nodal measurements are presented in Figure 1 and the Online Supplemental Data. The nodal degree and nodal efficiency of the left middle frontal gyrus (MFG) and bilateral inferior frontal gyrus, opercular part (IFGoperc) displayed significant decline between t3 and t1; in contrast, the nodal path length of these regions showed a significant increase between t3 and t1. Between t1 and t2 and between t2 and t3, only the region of the left IFGoperc presented significant alterations; that is, the nodal degree and nodal efficiency displayed reduction, whereas the nodal path length showed an increase at t2 compared with those at baseline and at t3 compared with those at t2. In addition, the right superior parietal gyrus exhibited a significant reduction in nodal efficiency between t1 and t2, and between t1 and t3. The nodal clustering coefficients of all the regions remained stable over time (data not shown).

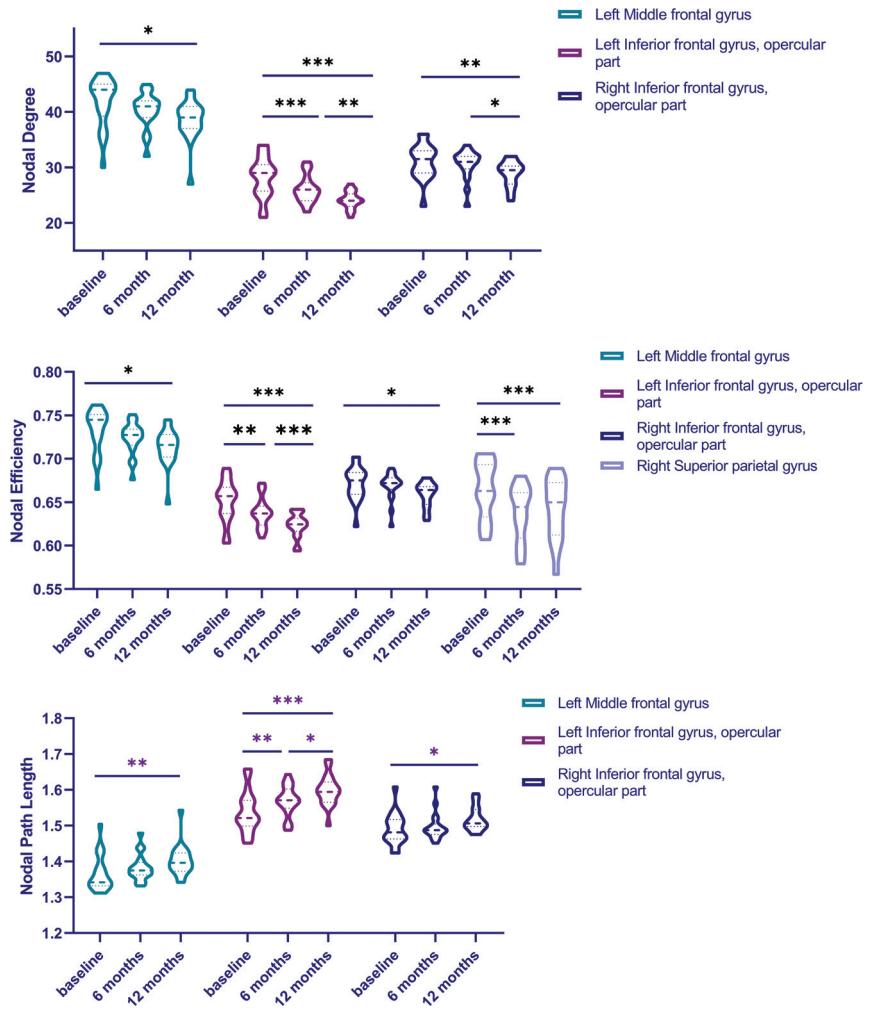

FIG 1. Plots of significant nodal network measurements of MS at different time points. *$P < .05$; **$P < .01$; ***$P < .001$.

Association between Network Measurements and EDSS

A series of correlations were analyzed to further explore which type of measurement showed a significant association with EDSS. The regions significantly related to EDSS are shown in Figure 2 and the Online Supplemental Data. All selected nodes were entered into the stepwise linear model. Only the nodal path length of the superior frontal gyrus, medial orbital part (ORBsupmed) was selected as a significant predictor for EDSS (Fig 3; Table 2).

DISCUSSION

In this study, we probed the brain changes in DTI and network measurements over a 1-year follow-up period in 18 patients with MS. The whole lesions (defined as all voxels of all lesions identified after WM lesion segmentation) and NAWM were chosen separately as the ROIs in the conventional diffusion measurement analysis. DTI measurements did not change significantly over the entire study period. While the network measurements showed significant alteration, and their clinical relevance with EDSS was also observed. Based on these findings, we speculated that the network measures may be used to monitor brain changes for MS during follow-up.

DTI Measurements

Brain changes within 1 year in MS as measured by using DTI remain inconclusive. Some research did not detect significant alterations of diffusion measurement in NAWM or lesions for MS during the 1-year follow-up period.[5,36-38] For example, Ontaneda et al[5] observed that the FA, MD, AD, and RD of NAWM remained stable during the 1-year follow-up period. Our study about diffusion measures can replicate their findings. However, some other studies did report significant progressive microstructural damage during their follow-up period,[39,40] which deviated from our findings. This may be attributed to the lower sample size, different MS subtypes included, analysis methods, or heterogeneous disease-modifying drugs used.

Structural WM Nodal Network Measurements

We detected topological changes in MS in several frontal brain regions in patients with MS. Compared with baseline, MS showed a significant decrease in the nodal degree and nodal efficiency and significant increase in the nodal path length in the left MFG and bilateral IFGoperc. Reduced nodal efficiency has been reported in previous studies on the MFG and IFGoperc for MS compared with healthy controls.[16] Our longitudinal studies extended this to a longitudinal period, as these regions exhibited significant changes during the 1-year follow-up period. The pathophysiological changes behind the reduced nodal efficiency may be related to the demyelination and axonal damage, which caused the disconnection between the nodes and eventually induced the lower efficiency of information transfer/communication.[41] Our findings indicate that the nodal degree, nodal efficiency, and nodal path length of the left MFG and bilateral IFGoperc could be used to monitor brain changes over time; moreover, these measurements may be developed as neuroimaging biomarkers to track brain changes in MS, but much more future work is needed. Specifically, the small sample size can be increased in future longitudinal studies, and prospective experiments should be performed. External validation could further verify their clinical values. Due to the small sample size, we could not differentiate between RRMS and SPMS. However, the results were almost stable when we excluded the 3 patients with SPMS (Online Supplemental Data). Another factor that may impact the findings was the disease-modifying treatment. However, we performed the subgroup analysis–the group was divided into 2 subgroups: high-efficiency group (patients who were stable) and low-efficiency group (patients who displayed

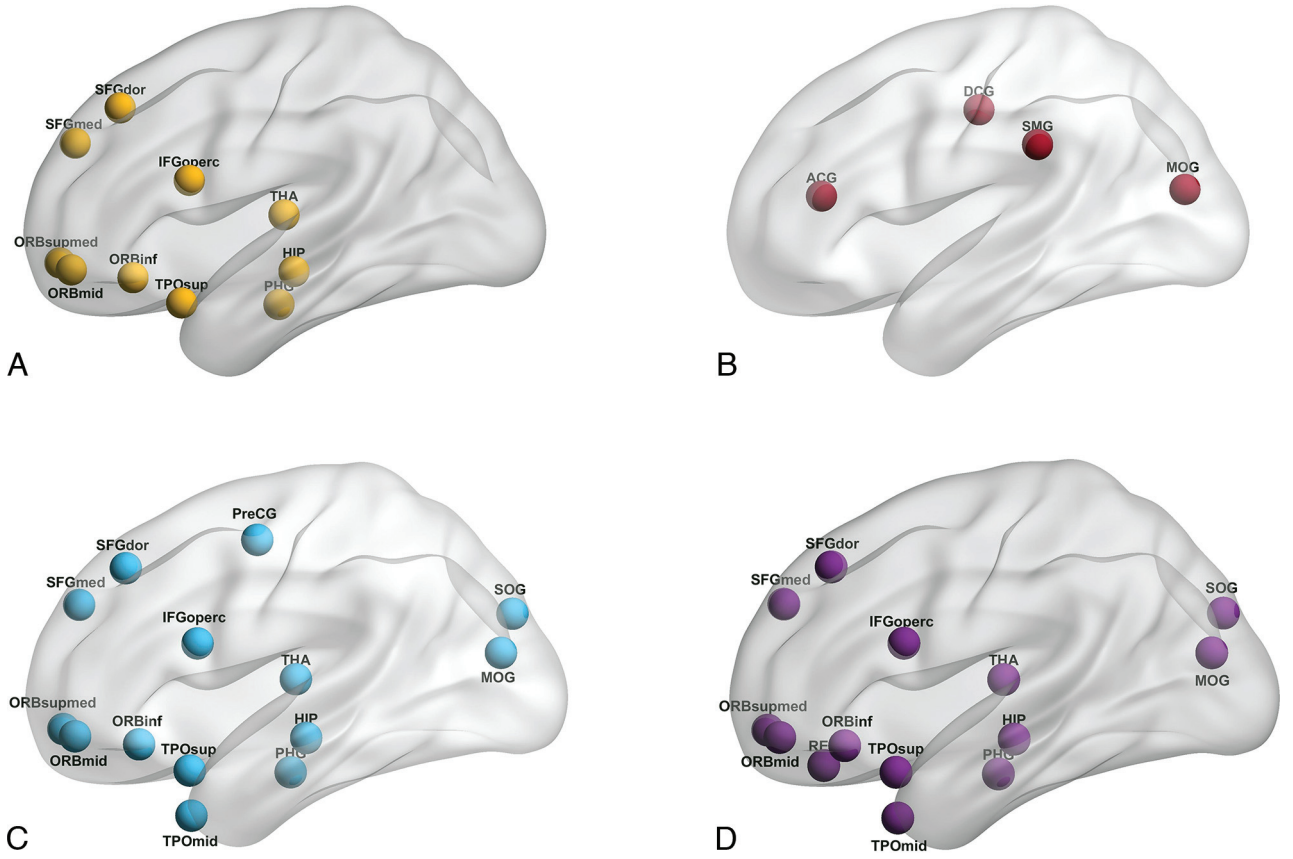

FIG 2. Three-dimensional graphs showed regions representing significant association with EDSS. *A*, Nodal degree. *B*, Nodal clustering coefficient. *C*, Nodal efficiency. *D*, Nodal path length. Brain region corresponding to the anatomical labels can be found in Automated Anatomical Labeling template.

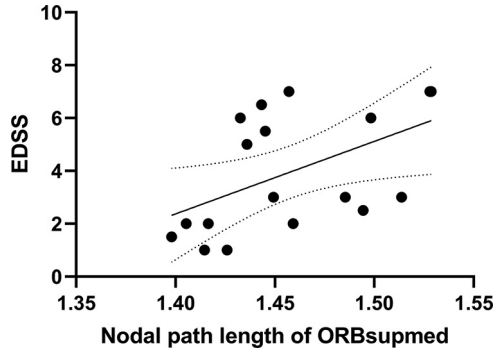

FIG 3. Plots of the stepwise linear regression between the nodal path length of superior frontal gyrus, medial orbital part (ORBsupmed), and baseline EDSS.

worsening, including MS02, MS04, MS06, MS07, and MS16). The results are presented in the Online Supplemental Data. We did not detect any significant difference between the 2 subgroups. This suggested that the disease-modifying treatment did not impact the findings.

In our analysis, statistically significant changes were not detected for the diffusion measurements. However, brain structural network measurements showed significant alterations compared with those at baseline. This suggests that conventional diffusion disruption and WM network reorganization may not share identical temporal patterns, indicating that network measurements could be used to monitor brain changes during follow-up.

Association between Network Measurements and EDSS

We further explored the relationship between the nodal measurements of all brain regions and EDSS. A multiple linear regression model was established between the nodal path length of ORBsupmed and EDSS, which indicated that it had the potential to be a promising predictor for EDSS. In a longitudinal MS study, Tsagkas et al[42] found that cortical thickness changes in the ORBsupmed region were significantly correlated with EDSS changes during the follow-up period, indicating a relationship between this brain region and EDSS. The underlying cytostructural mechanism may be related to the intralesional axonal loss and the following Wallerian degeneration. This eventually may cause the clinical disability. Similarly, these cytostructural changes may also cause the disconnection between the brain regions and increase the path length needed to information transfer. So, we were allowed to observe a positive relationship between nodal path length of ORBsupmed and EDSS.

Limitations

Our study still has some limitations. We did not recruit healthy controls; therefore, we could not track longitudinal changes in healthy individuals and were unable to compare the longitudinal differences between patients with MS and healthy controls. Future studies should also recruit healthy controls. Furthermore, our

Table 2: Selected linear regression model about EDSS

	Dependent Variable	R^2	Adjusted R^2	Regression Coefficient	95% CI	*P* Value
Model	EDSS(t1)	0.366	0.327	—	—	—
Constant	—	—	—	−46.625	[−81.89, −11.35]	.013
Nodal path length of ORBsupmed	—	—	—	34.231	[10.36, 58.10]	.008

Note:—The en dash indicates not applicable.

sample size was relatively small, and our findings may be viewed as preliminary and need confirmation in a larger cohort of MS. However, in this longitudinal study, each patient was examined and assessed 3 times, and the findings could still provide some clinical value.

CONCLUSIONS

The nodal degree, nodal efficiency, and nodal path length of the left MFG and bilateral IFGoperc may be used to monitor the brain changes over time in MS. The nodal path length of ORBsupmed could be used to evaluate physical disability in patients with MS. These findings together could elevate our understanding of MS.

Disclosure forms provided by the authors are available with the full text and PDF of this article at www.ajnr.org.

REFERENCES

1. Reich DS, Lucchinetti CF, Calabresi PA. **Multiple sclerosis.** *N Engl J Med* 2018;378:169–80 CrossRef Medline
2. Ge Y, Law M, Grossman RI. **Applications of diffusion tensor MR imaging in multiple sclerosis.** *Ann NY Acad Sci* 2006;1064:202–19 CrossRef Medline
3. Inglese M, Bester M. **Diffusion imaging in multiple sclerosis: research and clinical implications.** *NMR Biomed* 2010;23:865–72 CrossRef Medline
4. Soares JM, Marques P, Alves V, et al. **A hitchhiker's guide to diffusion tensor imaging.** *Front Neurosci* 2013;7:31 CrossRef Medline
5. Ontaneda D, Sakaie K, Lin J, et al. **Identifying the start of multiple sclerosis injury: a serial DTI study.** *J Neuroimaging* 2014;24:569–76 CrossRef Medline
6. Huang J, Liu Y, Zhao T, et al. **White matter microstructural alterations in clinically isolated syndrome and multiple sclerosis.** *J Clin Neurosci* 2018;53:27–33 CrossRef Medline
7. Klistorner A, Wang C, Yiannikas C, et al. **Evidence of progressive tissue loss in the core of chronic MS lesions: a longitudinal DTI study.** *Neuroimage Clin* 2018;17:1028–35 CrossRef Medline
8. Yu FF, Chiang FL, Stephens N, et al. **Characterization of normal-appearing white matter in multiple sclerosis using quantitative susceptibility mapping in conjunction with diffusion tensor imaging.** *Neuroradiology* 2019;61:71–79 CrossRef Medline
9. de Kouchkovsky I, Fieremans E, Fleysher L, et al. **Quantification of normal-appearing white matter tract integrity in multiple sclerosis: a diffusion kurtosis imaging study.** *J Neurol* 2016;263:1146–55 CrossRef Medline
10. Rubinov M, Sporns O. **Complex network measures of brain connectivity: uses and interpretations.** *Neuroimage* 2010;52:1059–69 CrossRef Medline
11. Fleischer V, Radetz A, Ciolac D, et al. **Graph theoretical framework of brain networks in multiple sclerosis: a review of concepts.** *Neuroscience* 2019;403:35–53 CrossRef Medline
12. Van Essen DC. **A tension-based theory of morphogenesis and compact wiring in the central nervous system.** *Nature* 1997;385:313–18 CrossRef Medline
13. Newman ME. **Modularity and community structure in networks.** *Proc Natl Acad Sci USA* 2006;103:8577–82 CrossRef Medline
14. Llufriu S, Martinez-Heras E, Solana E, et al. **Structural networks involved in attention and executive functions in multiple sclerosis.** *Neuroimage Clin* 2017;13:288–96 CrossRef Medline
15. Kocevar G, Stamile C, Hannoun S, et al. **Graph theory-based brain connectivity for automatic classification of multiple sclerosis clinical courses.** *Front Neurosci* 2016;10:478 CrossRef Medline
16. Shu N, Liu Y, Li K, et al. **Diffusion tensor tractography reveals disrupted topological efficiency in white matter structural networks in multiple sclerosis.** *Cereb Cortex* 2011;21:2565–77 CrossRef Medline
17. Hawkins R, Shatil AS, Lee L, et al. **Reduced global efficiency and random network features in patients with relapsing-remitting multiple sclerosis with cognitive impairment.** *AJNR Am J Neuroradiol* 2020;41:449–55 CrossRef Medline
18. Welton T, Constantinescu CS, Auer DP, et al. **Graph theoretic analysis of brain connectomics in multiple sclerosis: reliability and relationship with cognition.** *Brain Connect* 2020;10:95–104 CrossRef Medline
19. Charalambous T, Tur C, Prados F, et al. **Structural network disruption markers explain disability in multiple sclerosis.** *J Neurol Neurosurg Psychiatry* 2019;90:219–26 CrossRef Medline
20. Thompson AJ, Banwell BL, Barkhof F, et al. **Diagnosis of multiple sclerosis: 2017 revisions of the McDonald criteria.** *Lancet Neurol* 2018;17:162–73 CrossRef Medline
21. Lublin FD, Coetzee T, Cohen JA, International Advisory Committee on Clinical Trials in MS, et al. **The 2013 clinical course descriptors for multiple sclerosis.** *Neurology* 2020;94:1088–92 CrossRef Medline
22. Schmidt P. *Bayesian inference for structured additive regression models for large-scale problems with applications to medical imaging*, Dissertation, LMU München: Faculty of Mathematics, Computer Science and Statistics 2017
23. Schmidt P, Gaser C, Arsic M, et al. **An automated tool for detection of FLAIR-hyperintense white-matter lesions in multiple sclerosis.** *Neuroimage* 2012;59:3774–83 CrossRef Medline
24. Battaglini M, Jenkinson M, De Stefano N. **Evaluating and reducing the impact of white matter lesions on brain volume measurements.** *Hum Brain Mapp* 2011;33:2062–71 CrossRef Medline
25. Smith SM, Jenkinson M, Woolrich MW, et al. **Advances in functional and structural MR image analysis and implementation as FSL.** *Neuroimage* 2004;23 Suppl 1:S208–19 CrossRef Medline
26. Jenkinson M, Beckmann CF, Behrens TE, et al. **FSL.** *NeuroImage* 2012;62:782–90 CrossRef Medline
27. Tzourio-Mazoyer N, Landeau B, Papathanassiou D, et al. **Automated anatomical labeling of activations in SPM using a macroscopic anatomical parcellation of the MNI MRI single-subject brain.** *Neuroimage* 2002;15:273–89 CrossRef Medline
28. Gong G, He Y, Concha L, et al. **Mapping anatomical connectivity patterns of human cerebral cortex using in vivo diffusion tensor imaging tractography.** *Cereb Cortex* 2009;19:524–36 CrossRef Medline
29. Liu Y, Duan Y, Dong H, et al. **Disrupted module efficiency of structural and functional brain connectomes in clinically isolated syndrome and multiple sclerosis.** *Front Hum Neurosci* 2018;12:138 CrossRef Medline
30. Wang R, Benner T, Sorensen AG, et al. **Diffusion toolkit: a software package for diffusion imaging data processing and tractography.** *Proc Intl Soc Mag Reson Med* 2007;15

31. Mori S, Crain BJ, Chacko VP, et al. **Three-dimensional tracking of axonal projections in the brain by magnetic resonance imaging.** *Ann Neurol* 1999;45:265–69
32. Basser PJ, Pajevic S, Pierpaoli C, et al. **In vivo fiber tractography using DT-MRI data.** *Magn Reson Med* 2000;44:625–32 CrossRef
33. Shu N, Duan Y, Xia M, et al. **Disrupted topological organization of structural and functional brain connectomes in clinically isolated syndrome and multiple sclerosis.** *Sci Rep* 2016;6:29383 CrossRef Medline
34. Xu X, Lau KK, Wong YK, et al. **The effect of the total small vessel disease burden on the structural brain network.** *Sci Rep* 2018;8:7442 CrossRef Medline
35. Wang J, Wang X, Xia M, et al. **GRETNA: a graph theoretical network analysis toolbox for imaging connectomics.** *Front Hum Neurosci* 2015;9:386
36. Schneider R, Genc E, Ahlborn C, et al. **Temporal dynamics of diffusion metrics in early multiple sclerosis and clinically isolated syndrome: a 2-year follow-up tract-based spatial statistics study.** *Front Neurol* 2019;10:1165 CrossRef Medline
37. Zivadinov R, Bergsland N, Hagemeier J, et al. **Effect of teriflunomide on gray and white matter brain pathology in multiple sclerosis using volumetric and diffusion-tensor imaging MRI measures.** *J Neurol Sci* 2018;388:175–81 CrossRef Medline
38. Rashid W, Hadjiprocopis A, Davies G, et al. **Longitudinal evaluation of clinically early relapsing-remitting multiple sclerosis with diffusion tensor imaging.** *J Neurol* 2008;255:390–97 CrossRef Medline
39. Toschi N, De Santis S, Granberg T, et al. **Evidence for progressive microstructural damage in early multiple sclerosis by multi-shell diffusion magnetic resonance imaging.** *Neuroscience* 2019;403:27–34 CrossRef Medline
40. Fox RJ, Cronin T, Lin J, et al. **Measuring myelin repair and axonal loss with diffusion tensor imaging.** *AJNR Am J Neuroradiol* 2011;32:85–91 CrossRef Medline
41. Lemus HN, Warrington AE, Rodriguez M. **Multiple sclerosis.** *Neurol Clin* 2018;36:1–11 CrossRef Medline
42. Tsagkas C, Chakravarty MM, Gaetano L, et al. **Longitudinal patterns of cortical thinning in multiple sclerosis.** *Hum Brain Mapp* 2020;41:2198–215 CrossRef Medline